

Influence of Host Lattice on the Chemical Bonding Nature of Guest Species in High- T_c Superconducting $\text{I-Bi}_2\text{Sr}_{1.5-x}\text{La}_x\text{Ca}_{1.5}\text{Cu}_2\text{O}_y$ Nanohybrids

Seong-Ju Hwang,^{*,†} Dae Hoon Park,[†] and Jin-Ho Choy[‡]

Department of Applied Chemistry, Center for Optoelectronic and Microwave Devices, College of Natural Sciences, Konkuk University Chungju Campus, Chungju, Chungbuk 380-701, Korea, and National Nanohybrid Materials Laboratory, School of Chemistry, Seoul National University, Seoul 151-747, Korea

Received: May 16, 2004

The influence of the host lattice on the chemical bonding nature of guest iodine species in high- T_c superconducting $\text{I-Bi}_2\text{Sr}_{1.5-x}\text{La}_x\text{Ca}_{1.5}\text{Cu}_2\text{O}_y$ nanohybrids has been examined by performing combinative X-ray photoelectron spectroscopic (XPS) and X-ray absorption spectroscopic (XAS) analyses. The iodine species were found to possess two kinds of oxidation states, negatively charged iodine (I^{0-}) and highly oxidized heptavalent iodine (I^{+VII}). The concentration of heptavalent iodine species is significantly increased by replacing Sr^{+II} ions with La^{+III} ions, indicating that excess oxygen in the host lattice oxidizes the intercalated iodine into heptavalent iodine species. From mass spectroscopic analysis for disintercalated species, it is certain that the heptavalent iodine exists as a periodate IO_4^- cluster in easily removable sites such as the edge or surface of crystallite. The I L_{1-} edge XAS analyses reveal that even in heavily La-substituted compounds the content of the negatively charged iodide species is still greater than that of the periodate species. The degree of charge transfer between host and guest is also found to depend on La content, which makes it possible to explain the T_c behavior of iodine intercalates with respect to La substitution. The present study provides an intriguing example for the possible control of the bonding nature of guest species through a modification of the composition of the host lattice.

Introduction

The recent progress in nanotechnology has renewed research interest in intercalation chemistry, since it can provide an effective method to prepare nanoparticles or nanohybrids through an exfoliation process.^{1,2} In addition to such synthetic aspects, an intercalation technique allows us to examine the validity of theoretical models predicting a role of dimensionality in the physicochemical properties of low dimensional materials. In this context, the intercalation of guest species into the two-dimensional lattice of a high- T_c superconductor has attracted intense attention since it can give insight for the mechanism responsible for high- T_c superconductivity in copper oxides.^{3–6} Previously, we have developed several new high- T_c superconducting nanohybrids and invented a novel route to fabricate the thin film and wire of Bi-based cuprate superconductor through the intercalation of organic chain molecules followed by an exfoliation process.^{6–10} Among the known high- T_c superconducting nanohybrids, the iodine intercalation compound has been the most investigated system because of its facile preparation procedure, its relatively simple crystal structure, an availability of single crystalline samples, and so on. The iodine intercalation was reported to cause a slight decrease of T_c for the pristine bismuth cuprates. First, such a T_c change was explained by the weakening of interlayer coupling through the increase in interlayer distance.^{3,11} However, the presence of charge transfer between host and guest has been clarified by several spectroscopic studies.^{12–15} On the basis of these results, attempts have

been made to understand the T_c variation upon intercalation in terms of a change of hole density in superconductive CuO_2 sheets. Since the pristine $\text{Bi}_2\text{Sr}_2\text{CaCu}_2\text{O}_y$ possesses an overdoped hole concentration, a negatively charged iodide state would give rise to a T_c decrease through an increase in hole density in CuO_2 layers. On the contrary, the positive oxidation state of iodine can induce a decrease in hole density and therefore T_c of the pristine $\text{Bi}_2\text{Sr}_2\text{CaCu}_2\text{O}_y$ should be enhanced from the viewpoint of the charge-transfer effect. In such a case, the reported T_c depression upon iodine intercalation can be regarded as strong evidence of the significant contribution of interlayer coupling to the high-temperature superconductivity of Bi-based cuprate. However, there were some controversies about the bonding state of intercalated iodine species. Even though several types of oxidation states, such as I_2 , I_3^- , I^- , and I^{+VII} , have been suggested for the intercalated iodine species,^{12–16} the exact formation condition for each state has not been studied. In particular, special attention should be paid to the highly oxidized heptavalent iodine species that can result in a significant change in the hole density of CuO_2 sheets even at a small concentration. In this context, it is very important to elucidate the exact bonding state of intercalant species in probing the role of dimensionality in the high- T_c superconductivity of this nanohybrid system. We have postulated that such an inconsistency about the oxidation state of intercalated iodine among the previous reports would originate from the discrepancy of the host composition used. In this regard, we have systematically investigated the influence of the host lattice on the chemical bonding nature of intercalated iodine species. For this purpose, we have controlled oxygen content and the hole density of the CuO_2 layer through a substitution of La^{+III} ions for Sr^{+II} ions.^{17–19} We have applied complementarily I 3d X-ray photoelectron spectroscopic (XPS)

* To whom all correspondences should be addressed. Tel: +82-43-840-3569. Fax: +82-43-851-4169. E-mail: hwangsj@kku.ac.kr.

[†] Konkuk University Chungju Campus.

[‡] Seoul National University.

and I L_i-edge X-ray absorption near edge structure (XANES) analyses not only in order to elucidate the oxidation state and bonding site of iodine intercalant, but also to clarify an origin of T_c variation upon intercalation. In addition, the chemical identity and thermal stability of intercalated iodine have been examined by performing mass spectroscopic analysis for the disintercalated species during thermal analysis.

Experimental section

The polycrystalline samples of $\text{Bi}_2\text{Sr}_{1.5-x}\text{La}_x\text{Ca}_{1.5}\text{Cu}_2\text{O}_y$ ($0 \leq x \leq 0.4$) were synthesized by the conventional solid-state reaction and used as host materials for the intercalation of iodine.^{17–20} The single phasic intercalates of iodine were obtained by heating the pristine polycrystals with an excess amount of guest molecules in an evacuated silica tube at 180 °C for iodine. The formation of the first-staged iodine intercalates $\text{IBi}_2\text{Sr}_{1.5-x}\text{La}_x\text{Ca}_{1.5}\text{Cu}_2\text{O}_y$ was confirmed by powder X-ray diffraction (XRD) analyses. The evolution of superconductivity upon intercalation was examined by dc magnetic susceptibility measurements. The dc magnetic susceptibilities were measured as a function of temperature with a superconducting quantum interference device (SQUID) magnetometer, where the applied magnetic field was 20 Oe. XPS spectra were recorded with a PHI 5100 Perkin-Elmer spectrometer. The binding energies (BE) were obtained with an accuracy of 0.8 eV and by charge referencing to an adventitious C 1s peak at 284.6 eV. To discriminate the bonding sites of intercalated iodine species, XPS spectra were also measured after the sputtering of Ar^+ ion with an energy of 2 keV. The present X-ray absorption spectra (XAS) were measured at room temperature for powdered samples in a transmission mode. The XAS experiments were performed at the beam line 7C at the Photon Factory, National Laboratory for High Energy Physics in Tsukuba, operated at 2.5 GeV and 260–370 mA.²¹ The samples were finely ground, mixed with boron nitride (BN) in an appropriate ratio, and pressed into pellets in order to obtain an optimum absorption jump ($\Delta\mu \cdot t \cong 1$) enough to be free from the thickness and pinhole effects.^{22,23} The X-ray was monochromatized by the silicon (111) double crystal monochromator detuned to 60% of the maximum intensity to minimize the higher harmonics for I L_i-edge. The data analysis for the present spectra was performed by standard procedure as reported previously.⁷

Results and Discussion

The powder XRD patterns for the pristine $\text{Bi}_2\text{Sr}_{1.5-x}\text{La}_x\text{Ca}_{1.5}\text{Cu}_2\text{O}_y$ ($0 \leq x \leq 0.4$) and their iodine-intercalates are presented in Figure 1. Upon iodine intercalation, all the (00 l) reflections are shifted to lower angles, indicating a lattice expansion along the c -axis. From the least-squares fitting analysis, an increase of the c -axis lattice parameter is determined to be about 7.0–7.1 Å for the iodine intercalates over all the present La substitution range, as listed in Table 1. This confirms the formation of the first-staged intercalates regardless of La substitution rate. It is also found that the c -axis parameter for all the present compounds decreases continuously as the x value increases. This can be understood by the fact that the Sr^{+II} ion is replaced partly by the relatively smaller La^{+III} ion (Sr^{+II} (12) = 1.25 Å, La^{+III} (12) = 1.50 Å, where the number in parentheses represents the coordination number).²⁴ On the contrary, the inplane lattice parameter is slightly enhanced by La substitution, which is attributable to the reduction of Cu oxidation state resulting in an elongation of (Cu–O) bond distances. As a result of such variations of lattice parameters, the overlapped (0010)/

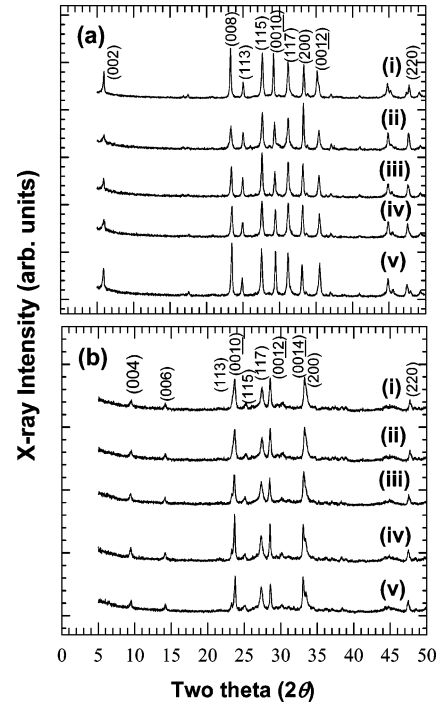


Figure 1. Powder XRD patterns for (a) the pristine $\text{Bi}_2\text{Sr}_{1.5-x}\text{La}_x\text{Ca}_{1.5}\text{Cu}_2\text{O}_y$ and (b) their iodine-intercalates with the La content (x) of (i) 0, (ii) 0.1, (iii) 0.2, (iv) 0.3, and (v) 0.4.

TABLE 1: Lattice Parameters, Unit Cell Volumes (V_c), and Crystal Symmetries of the Pristine $\text{Bi}_2\text{Sr}_{1.5-x}\text{La}_x\text{Ca}_{1.5}\text{Cu}_2\text{O}_y$ and Their Iodine Intercalates

sample	a (Å)	c (Å)	V_c	crystal symmetry
$\text{Bi}_2\text{Sr}_{1.5}\text{Ca}_{1.5}\text{Cu}_2\text{O}_y$	5.399	30.731	895.784	tetragonal
$\text{Bi}_2\text{Sr}_{1.4}\text{La}_{0.1}\text{Ca}_{1.5}\text{Cu}_2\text{O}_y$	5.401	30.591	892.364	tetragonal
$\text{Bi}_2\text{Sr}_{1.3}\text{La}_{0.2}\text{Ca}_{1.5}\text{Cu}_2\text{O}_y$	5.408	30.497	891.929	tetragonal
$\text{Bi}_2\text{Sr}_{1.2}\text{La}_{0.3}\text{Ca}_{1.5}\text{Cu}_2\text{O}_y$	5.414	30.408	891.301	tetragonal
$\text{Bi}_2\text{Sr}_{1.1}\text{La}_{0.4}\text{Ca}_{1.5}\text{Cu}_2\text{O}_y$	5.418	30.360	891.209	tetragonal
$\text{IBi}_2\text{Sr}_{1.5}\text{Ca}_{1.5}\text{Cu}_2\text{O}_y$	5.393	37.685	1096.047	tetragonal
$\text{IBi}_2\text{Sr}_{1.4}\text{La}_{0.1}\text{Ca}_{1.5}\text{Cu}_2\text{O}_y$	5.395	37.612	1094.736	tetragonal
$\text{IBi}_2\text{Sr}_{1.3}\text{La}_{0.2}\text{Ca}_{1.5}\text{Cu}_2\text{O}_y$	5.402	37.587	1096.849	tetragonal
$\text{IBi}_2\text{Sr}_{1.2}\text{La}_{0.3}\text{Ca}_{1.5}\text{Cu}_2\text{O}_y$	5.412	37.567	1100.328	tetragonal
$\text{IBi}_2\text{Sr}_{1.1}\text{La}_{0.4}\text{Ca}_{1.5}\text{Cu}_2\text{O}_y$	5.418	37.482	1100.274	tetragonal

(113) and (0014)/(200) reflections are split into two features for the iodine intercalates with high La content (Figure 1).

To probe the variation of T_c upon intercalation, dc magnetic susceptibility was measured as a function of temperature for the pristine compounds and their iodine intercalates. Figure 2 displays the plot of T_c vs the La substitution rate (x) before and after intercalation. For the pristine compounds, the T_c dependence on x exhibits a parabolic feature with a maximum T_c at $x = 0.1$ – 0.2 , as observed for the T_c – x curve of yttrium-substituted $\text{Bi}_2\text{Sr}_2\text{Ca}_{1-x}\text{Y}_x\text{Cu}_2\text{O}_y$.²⁵ According to the previous report on the relation between T_c and hole concentration in the cation-substituted Bi-based cuprate system,^{17,25,26} T_c increases to a maximum at an optimum hole concentration and then decreases even though the hole concentration decreases monotonically with the La substitution. Such results imply that there are two regions (hole overdoped and underdoped regions) with an optimum hole concentration where the maximum T_c appears. Therefore, our T_c vs x plot for the pristine compounds indicates that the region at $x < 0.1$ is an overdoped state and the region $x = 0.1$ – 0.2 is an optimally doped one, while the region above 0.2 is an underdoped one. Upon iodine intercalation, T_c decreases by ~ 13 K in the overdoped region with $x = 0$ but increases by about 4–5 K in the underdoped region with $0.3 \leq x \leq 0.4$. It

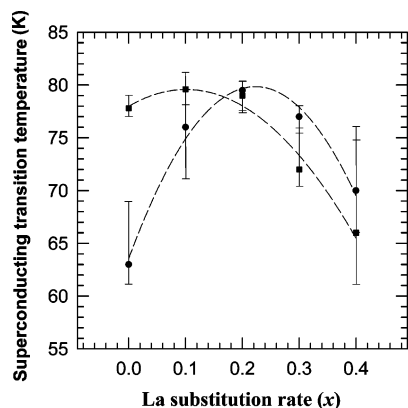


Figure 2. Superconducting transition temperature vs La substitution rate (x) plots for the pristine $\text{Bi}_2\text{Sr}_{1.5-x}\text{La}_x\text{Ca}_{1.5}\text{Cu}_2\text{O}_y$ (squares) and their iodine intercalates (circles). The dashed parabolae obtained from the interpolation of data are guides for the eyes. The upper and lower limits of error bars denote the temperature at which the diamagnetic signals correspond to 1 and 10% of the values at 5 K, respectively.

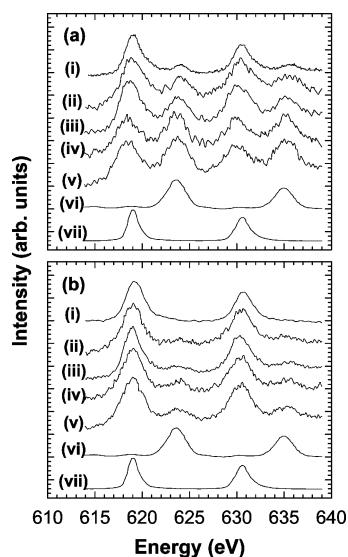


Figure 3. (a) I 3d XPS spectra for the iodine intercalated $\text{Bi}_2\text{Sr}_{1.5-x}\text{La}_x\text{Ca}_{1.5}\text{Cu}_2\text{O}_y$ with the La content (x) of (i) 0, (ii) 0.1, (iii) 0.2, (iv) 0.3, (v) 0.4, and the references (vi) KIO_4 and (vii) KI, and (b) the corresponding spectra after Ar^+ -ion sputtering for 60 s.

is worth noting here that the optimum substitution concentration of $x = 0.1$ at $T_c = T_c^{\text{max}}$ for the pristine compound is shifted to $x \cong 0.2$ upon iodine intercalation. This suggests that T_c variation is mainly ascribed to a charge transfer between host and guest leading to a change of hole concentration upon iodine intercalation. If there is a considerable contribution of interlayer coupling to high- T_c superconductivity of the host material, the T_c^{max} observed for optimum hole concentration should be markedly depressed by the intercalation process due to a weakening of interlayer interaction. However, as shown in Figure 2, the maximum T_c is found to remain nearly the same before and after intercalation. This underlines a negligible contribution of interlayer coupling to the high-temperature superconductivity of bismuth cuprates. To investigate the direction and degree of charge transfer upon iodine intercalation, we have examined the oxidation state of intercalated iodine species by using XPS and XAS analyses.

I 3d XPS spectra of iodine intercalated $\text{Bi}_2\text{Sr}_{1.5-x}\text{La}_x\text{Ca}_{1.5}\text{Cu}_2\text{O}_y$ ($0 \leq x \leq 0.4$) are presented in Figure 3, in comparison with those of references KI and KIO_4 . There are two sets of spin-doublets for all the present spectra, suggesting the presence of

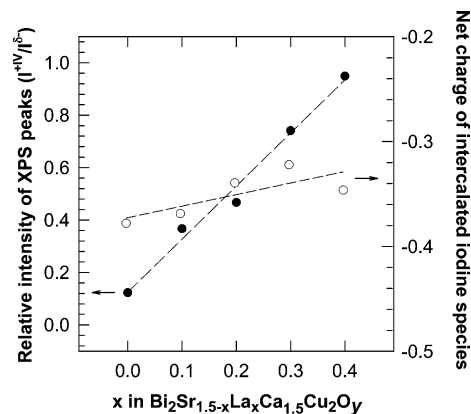


Figure 4. The relative intensity of XPS peaks corresponding to $\text{I}^{+\text{VII}}/\text{I}^{0-}$ species (closed circles) and the net charge of intercalated iodine species (open circles) as a function of La content (x). The dashed lines obtained from the interpolation of data are guides for the eyes.

two kinds of iodine species with different oxidation states. A comparison of the present spectra with the reference ones reveals that the main doublet at around 619 and 630.4 eV corresponds to negatively charged iodine species while the other doublet at higher energies of 623.9 and 635.3 eV originates from highly oxidized heptavalent ($\text{I}^{+\text{VII}}$) species.²⁷ However, it is worthwhile to mention here that the small BE difference between the negatively charged iodide anion (618.0–619.5 eV) and neutral iodine (619.9 eV) prevent us from conclusively assigning the lower BE features as a specific oxidation state.²⁷ The areas of the observed XPS peaks were estimated by convoluting the spectra with Lorentzian functions. The obtained peak areas are plotted in Figure 4 as a function of La content. The ratio of $\text{I}^{+\text{VII}}/\text{I}^{0-}$ is remarkably enhanced by replacing $\text{Sr}^{+\text{II}}$ with $\text{La}^{+\text{III}}$. This is a very intriguing example for the effect of host composition on the chemical bonding nature of guest species. Generally such an aliovalent substitution of $\text{Sr}^{+\text{II}}$ with $\text{La}^{+\text{III}}$ has two significant influences on the electronic structure and composition of the host lattice, that is, (1) a decrease of hole density in the CuO_2 layer and (2) an increase of the oxygen content of the host lattice, which is induced by an increase of cationic charge.¹⁸ Judging from the fact that the existence of the highly oxidized heptavalent iodine species implies an electron transfer from the guest to the host lattice during the intercalation process, a decrease of Cu oxidation state caused by La substitution (i.e., the effect of (1)) would be unfavorable for creation of such highly oxidized species. In this regard, an increase of oxygen content in the host lattice (i.e., the effect of (2)) would play a crucial role in forming the heptavalent iodine species. Hence, this species would exist in the form of a periodate (IO_4^-) cluster created by the reaction between iodine and oxygen. This conclusion is further supported by the I 3d XPS result for the iodine intercalate of oxygen-rich bismuth cuprate with $x = 0$,²⁸ in which a greater spectral weight is observed for the higher BE peaks corresponding to periodate species than the lower BE peaks (not shown here). This shows the important role of excess oxygen in forming highly oxidized iodine species. On the other hand, the present XPS results on $\text{I}-\text{Bi}_2\text{Sr}_{1.5-x}\text{La}_x\text{Ca}_{1.5}\text{Cu}_2\text{O}_y$ seem to suggest a reversal of the direction of charge transfer upon replacement of an $\text{Sr}^{+\text{II}}$ ion with an $\text{La}^{+\text{III}}$ ion. That is, Bi-based cuprate with little La content would donate a fraction of an electron to the intercalated iodine layer whereas heavily La-substituted Bi-based cuprate would accept electrons from iodine leading to formation of heptavalent iodine. However, considering the fact that XPS is sensitive mainly to surface species, the bonding state of iodine in the

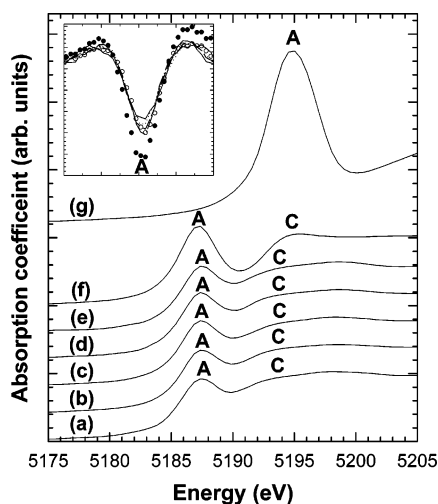


Figure 5. I L_1 -edge XANES spline spectra for the iodine intercalated $\text{Bi}_2\text{Sr}_{1.5-x}\text{La}_x\text{Ca}_{1.5}\text{Cu}_2\text{O}_y$ with the La content (x) of (a) 0 (solid lines), (b) 0.1 (dotted lines), (c) 0.2 (dashed lines), (d) 0.3 (dot-dashed lines), and (e) 0.4 (open circles), together with the reference spectra of (f) I_2 (closed circles) and (g) KIO_4 . The information in parentheses is for the curves in the inset. The inset provides enlarged views of the second derivative spectra with an energy range of 5183–5191 eV.

bulk state should be further studied. In this regard, we have probed the effect of Ar^+ ion sputtering on XPS spectra. As shown in Figure 3b, the higher BE peaks are almost eliminated by Ar^+ ion sputtering for 60 s whereas the lower BE ones are remarkably enhanced. Two origins of spectral variation after Ar ion sputtering can be proposed. One is a reduction of highly oxidized species under high vacuum chamber and the other is an elimination of easily removable species on the grain boundary or surface. However, based only on the XPS results, we were unable to conclusively assign the main mechanism of spectral change upon Ar sputtering. To solve this problem, we have performed I L_1 -edge XANES spectroscopy that can sensitively reflect the iodine species in the bulk.

The I L_1 -edge XANES spline and second derivative spectra for the iodine intercalated $\text{IBi}_2\text{Sr}_{1.5-x}\text{La}_x\text{Ca}_{1.5}\text{Cu}_2\text{O}_y$ ($0 \leq x \leq 0.4$) are represented in Figure 5, in comparison with those for free I_2 and KIO_4 . The spectral features of iodine intercalates are found to be nearly the same as those of a free I_2 molecule, except for a slight depression of the white line peak A corresponding to the transition from the $2s$ core level to unoccupied $5p$ states.²⁰ On the contrary, there are no spectral similarities between the spectra of iodine intercalates and KIO_4 . Especially, no trace of white line peak A is observed near 5195 eV for all the present intercalates. Considering the fact that the XAS spectrum is dependent mainly on the bulk species, the present results show that only a small amount of periodate is stabilized on the edge or surface of crystallites. On the other hand, since the intensity of the white line peak sensitively reflects the density of unoccupied final states,²⁰ the average oxidation state of intercalated iodine can be precisely deduced from the modification of peak intensity upon intercalation. As can be seen clearly from the inset of Figure 5, the intensity of the peak A for the iodine intercalates is somewhat depressed compared to that for solid iodine, which signals that the unoccupied $5p$ orbital is partially filled with the electron transferred from the host lattice. The area of the white line feature was determined by convoluting the spline spectra with Lorentzian and sigmoidal functions. The net charge of intercalated iodine species was calculated from the relative peak areas of iodine intercalates and neutral iodine; see Figure 4. The area of the white line peak is found to be ~ 33 –37% smaller for

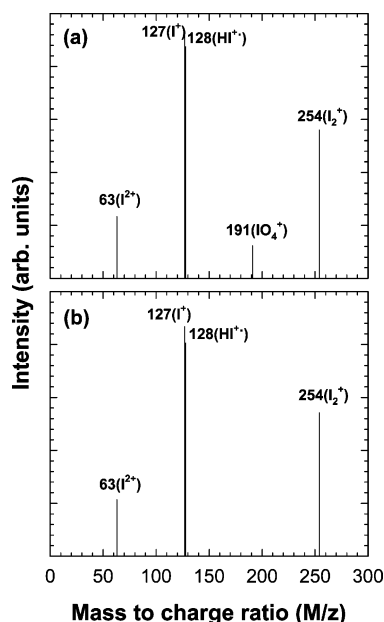


Figure 6. Mass spectra of the disintercalated iodine species during thermal analysis at (a) 180 and (b) 400 °C.

the iodine intercalates than for neutral iodine, suggesting the presence of nearly one hole per three iodine atoms. This is well consistent with micro-Raman results indicating the presence of triiodide (I_3^-) anions in the iodine intercalate.^{14,15} A closer inspection on the inset of Figure 5 reveals that the intensity of this peak increases slightly but distinctly by replacing Sr^{+II} with La^{+III} , underlining that the degree of charge transfer between host and guest is dependent on the composition of the host compound. Such a variation of white line intensity upon La substitution would be attributed to the formation of highly oxidized iodine species, leading on average to an enhancement of I $5p$ hole density of the intercalated iodine layer.

Additional information about the bonding state of intercalated iodine species has been obtained from the thermogravimetry–evolved gas analysis (TGA–EGA) for the iodine intercalate of related bismuth cuprate ($\text{IBi}_{2-x}\text{Pb}_x\text{Sr}_2\text{Ca}_2\text{Cu}_3\text{O}_y$).²⁹ From XPS study for this sample, intense higher BE peaks corresponding to I^{+VII} species are also observed, such as heavily La-substituted $\text{IBi}_2\text{Sr}_{1.5-x}\text{La}_x\text{Ca}_{1.5}\text{Cu}_2\text{O}_y$ (not shown here). The mass spectra of disintercalated guest species evolved at 180 and 400 °C are illustrated in Figures 6a and b, respectively. The main cationic species are determined to be I^{2+} , I^+ , HI^{+} , and I_2^+ with the mass-to-charge (M/Z) ratios of 63, 127, 128, and 254, which would originate from disintercalated triiodide molecules. In addition to these species, an oxygenated IO_4^+ cluster with $M/Z = 191$ is discernible from the spectrum measured at 180 °C, but not from the spectrum at 400 °C. These results support the above conclusion that the heptavalent iodine is stabilized as an oxygenated periodate species with lower thermal stability, compared to the negatively charged triiodide species.

On the basis of the present experimental findings, it is concluded that the concentration of highly oxidized heptavalent iodine species depends on the host composition and this species is mainly located in the easily removable sites. It is certain that the average oxidation state of guest iodine species and the degree of charge transfer between host and guest can be controlled by modification of the host lattice composition. Based on the present findings, we can explain the T_c variation of iodine intercalates upon La substitution from the viewpoint of the charge-transfer effect. As shown in Figure 2, the T_c increase in the underdoped region (i.e., higher La content) is found to be

less prominent than the T_c decrease in the overdoped region. This can be understood from the variation of the iodine oxidation state probed by XPS and XANES analyses. That is, the iodine intercalate with high La substitution rate possesses more periodate species and hence fewer holes are transferred into CuO_2 sheets upon iodine intercalation, resulting in a less prominent T_c change.

Conclusion

In this work, we have found a close relationship between the oxidation state of intercalated iodine and the composition of the host $\text{Bi}_2\text{Sr}_{1.5-x}\text{La}_x\text{Ca}_{1.5}\text{Cu}_2\text{O}_y$ lattice. The increase of oxygen content in the host lattice by La substitution enhances the concentration of heptavalent periodate (IO_4^-), even though the majority of intercalated iodine is stabilized as a triiodide anion regardless of the La substitution rate. Such a variation of iodine oxidation state allows us to explain the T_c behavior of iodine intercalates with respect to La substitution on the basis of charge-transfer effect. The T_c^{max} for optimum hole concentration is found to remain nearly the same before and after intercalation, highlighting a negligible contribution of interlayer coupling to the high-temperature superconductivity of bismuth cuprates. The present results can be regarded as a unique example of the controllable oxidation state of intercalated species through a modification of the chemical formula of the host lattice. Based on this finding, we can suggest a possible optimization of the useful properties of the intercalant layer in various nanohybrids (e.g., superionic conducting $\text{AgI-Bi}_2\text{Sr}_{1.5-x}\text{La}_x\text{Ca}_{1.5}\text{Cu}_2\text{O}_y$) by selecting the appropriate host composition.

Acknowledgment. This work was supported by grant No. R08-2003-000-10409-0 from the Basic Research Program of the Korea Science & Engineering Foundation. The authors are grateful to Prof. M. Nomura for helping us to get the XAS data in the Photon Factory.

References and Notes

- (1) *Soft Chemistry Routes to New Materials-Chimie Douce*, International Symposium, Materials Science Forum; Vol. 152–153, 1994, and papers therein.
- (2) Wang, L.; Kanatzidis, M. G. *Chem. Mater.* **2001**, *13*, 3717. Hwang, S. J.; Petkov, V.; Rangan, K. K.; Shastri, S.; Kanatzidis, M. G. *J. Phys. Chem. B* **2002**, *106*, 12453.
- (3) Xiang, X. D.; McKernan, S.; Vareka, W. A.; Zettl, A.; Corkill, J. L.; Barbee, T. W., III; Cohen, M. L. *Nature* **1990**, *348*, 145.

- (4) Choy, J. H.; Hwang, S. J.; Hwang, S. H.; Lee, W.; Jung, D.; Lee, M.; Lee, H. J. *J. Phys. Chem. B* **2001**, *105*, 5174.
- (5) Yurgens, A.; Winkler, D.; Claesson, T.; Hwang, S. J.; Choy, J. H. *Physica C* **2001**, *362*, 286.
- (6) Choy, J. H.; Kwon, S. J.; Park, G. S. *Science* **1998**, *280*, 1589.
- (7) Choy, J. H.; Park, N. G.; Hwang, S. J.; Kim, D. H.; Hur, N. H. *J. Am. Chem. Soc.* **1994**, *116*, 11564; Choy, J. H.; Hwang, S. J.; Park, N. G. *J. Am. Chem. Soc.* **1997**, *119*, 1624.
- (8) Choy, J. H.; Kim, Y. I.; Hwang, S. J.; Muraoka, Y.; Ohnishi, N.; Hiraga, K.; Huong, P. V. *J. Phys. Chem. B* **2000**, *104*, 9086.
- (9) Choy, J. H.; Kim, Y. I.; Hwang, S. J.; Huong, P. V. *J. Phys. Chem. B* **2000**, *104*, 7273.
- (10) Choy, J. H.; Kwon, S. J.; Hwang, S. J.; Kim, Y. I.; Jang, E. S. *Int. J. Inorg. Mater.* **2001**, *3*, 253.
- (11) Xiang, X. D.; Vareka, W. A.; Zettl, A.; Corkill, J. L.; Barbee, T. W., III; Cohen, M. L.; Kijima, N.; Gronsky, R. *Science* **1991**, *254*, 1487.
- (12) Choy, J. H.; Kang, S. G.; Kim, D. H.; Hwang, S. J.; Itoh, M.; Inaguma, Y.; Nakamura, T. *J. Solid State Chem.* **1993**, *102*, 284.
- (13) Fujiwara, A.; Koike, Y.; Sanada, N.; Pooke, D.; Kishio, K.; Kitazawa, K.; Syono, Y.; Tachiki, M. *J. Phys. Chem. Solids* **1992**, *53*, 1589.
- (14) Faulques, E.; Russo, R. E. *Solid State Commun.* **1992**, *82*, 531.
- (15) Huong, P. V.; Verma, A. L. *Phys. Rev. B* **1993**, *48*, 9869.
- (16) Qiu, C. H.; Ahrenkiel, S. P.; Wada, N.; Cizek, T. F. *Physica C* **1991**, *185–189*, 825.
- (17) Agarwal, S. K.; Narlikar, A. V. *Prog. Cryst. Growth Character.* **1994**, *28*, 219.
- (18) Mitzi, D. B.; Lombardo, L. W.; Kapitulnik, A.; Laderman, S. S.; Jacowitz, R. D. *Phys. Rev. B* **1990**, *41*, 6564.
- (19) Choy, J. H.; Park, N. G.; Hwang, S. J.; Khim, Z. G. *J. Phys. Chem.* **1996**, *100*, 3783.
- (20) Hwang, S. J.; Park, N. G.; Kim, D. H.; Choy, J. H. *J. Solid State Chem.* **1998**, *138*, 66.
- (21) Oyanagi, H.; Matsushida, T.; Ito, M.; Kuroda, H. *KEK Report* **1984**, *83*, 30.
- (22) Lytle, F. W.; van der Laan, G.; Gregor, R. B.; Larson, E. M.; Violet, C. E.; Wong, J. *Phys. Rev. B* **1990**, *41*, 8955.
- (23) Stern, E. A.; Kim, K. *Phys. Rev. B* **1981**, *23*, 3781.
- (24) Shannon, R. D. *Acta Crystallogr., Sect. A* **1976**, *32*, 751.
- (25) Maeda, A.; Hase, M.; Tsukada, I.; Noda, K.; Takebayashi, S.; Uchinokura, K. *Phys. Rev. B* **1990**, *41*, 6418.
- (26) Manthiram, A.; Tang, X. X.; Goodenough, J. B. *Phys. Rev. B* **1990**, *42*, 138.
- (27) *Handbook of X-ray Photoelectron Spectroscopy*; Wagner, C. D.; Riggs, W. M.; Davis, L. E.; Moulder, J. H.; Muilenberg, G. E. Eds.; Perkin-Elmer Corp.: Eden Prairie, MN, 1979.
- (28) In the case of unsubstituted bismuth cuprate with $x = 0$, an oxygen-rich sample was also prepared by a slow cooling process from the sintering temperature (860 °C). Due to the overdoping of the hole, the T_c of the oxygen-rich sample was found to be 70 K, which is lower than that of the pristine sample.
- (29) In the course of thermal analysis, the iodine intercalate was heated from room temperature to 800 °C at a rate of 20 °C/min in a flowing Ar gas. The disintercalated chemical species during thermal analysis were analyzed by using a quadrupole mass spectrometer (electron impacting type EI, VG Scientific). The evolved gas was instantly introduced into the mass spectrometer through a flexible capillary. Energy of the impacting electron used in the mass spectrometer was 70 eV.